Kormilainen, Riku; Luomaniemi, Rasmus; Lehtovuori, Anu; Khripkov, Alexander; Ilvonen, Janne; Viikari, Ville

A Dual-Polarized Wideband Planar Multiport Mobile Antenna

Published in:
2022 16th European Conference on Antennas and Propagation, EuCAP 2022

DOI:
10.23919/EuCAP53622.2022.9769536

Published: 01/01/2022

Document Version
Peer-reviewed accepted author manuscript, also known as Final accepted manuscript or Post-print

A Dual-Polarized Wideband Planar Multiport Mobile Antenna

Riku Kormilainen*, Rasmus Luomaniemi*†, Anu Lehtovuori*, Alexander Khripkov†, Janne Ilvonen†, Ville Viikari*

*Department of Electronics and Nanoengineering, Aalto University, FI-00076 AALTO, Finland, riku.kormilainen@aalto.fi

†Huawei Technologies Finland, 00180 Helsinki, Finland

***Abstract*—Additional antennas are needed in smart phones to support 5G bands. The metal rim, which is the most attractive position for antennas, is already fully occupied by antennas supporting legacy bands. Therefore, there is a growing interest in new, more challenging antenna locations, such as the back cover of the phone. In this paper, we introduce a dual-polarized frequency reconfigurable wideband planar multiport antenna to the back cover of a mobile phone. The antenna has a height of only 0.5 mm. The simulations show that the introduced antenna achieves better than -5.8 dB efficiency from 3.3 GHz to 4.2 GHz.**

***Index Terms*—dual-polarized, multi-feed, multiport, planar antenna.**

I. Introduction

Modern mobile antennas are typically realized in the gap between the metal rim and the metallic main body of the smart phone [1]–[4]. The larger the gap (also called clearance), the better the radiation properties [5]. Because the rim area is already now fully occupied by antennas, additional 5G or other new antennas need to be realized on less attractive locations, such as in the back cover of the phone.

Different types of planar inverted F-antennas (PIFAs) have already been utilized [6], [7], and they can be placed over the ground plane. PIFAs are one type of patch antennas which are commonly used in a wide range of applications, but are not so popular in modern mobile phones. Traditionally, a simple patch antenna is narrowband, has a single linear polarization and employs a single feed. Efforts have been made to widen the bandwidth with varactor diodes [8]–[10] and to achieve multiple polarizations with pin diodes [11], [12] in the case of single feed patch antennas. There are also designs achieving both frequency and polarization reconfigurability [13], [14].

Besides single feed patch antennas, multiport solutions exist [15]–[22]. As an example, the dipole can be realized as a multiport antenna by feeding it with two differential ports, as done in [23]. Differential feeding is gaining popularity in patch antennas as well [15]–[17]. The multiport patch antenna solutions are not limited to two ports nor differential feeding, and they are used in various ways. In [18], [19], a single patch antenna has multiple ports, and they achieve four- and three-element multiple-input-multiple-output (MIMO) operations, respectively. Furthermore, the polarization can be changed from linear to circular with multiple feeds as shown in [20]. Even multiple different polarizations can be achieved when the antenna is fed with multiple ports. In [21], the proposed patch antenna achieves six different polarizations by changing the excitation coefficients of the ports, and in [22], the antenna is frequency reconfigurable besides having polarization diversity.

In this paper, we propose a novel multiport antenna with both frequency and polarization agility. Polarization agile operation is achieved by effectively feeding the antenna with two ports, and the frequency reconfigurability is possible with four tunable capacitors. The proposed antenna is intended to be used in sub-6 GHz 5G applications, and it achieves a band of 3.3–4.2 GHz with better than -5.8 dB efficiency. Unlike other frequency and polarization agile designs [13], [14], [22], the proposed design is part of a mobile phone. Other designs have substrate thickness of around 3 mm making it impossible to fit them inside a practical device. The thickness of our proposed design is only 0.5 mm so that it could be realized on the thin back cover of the device. This thickness makes it difficult to design antennas with good radiation properties since decreasing height increases substrate losses [24] and narrows the bandwidth [25] of planar microstrip antennas. In addition, the proposed antenna is located under a lossy substrate i.e. the back glass cover of the phone.

II. Antenna structure and operating principle

Current distribution can be excited more selectively with multiple feeds, which makes it possible to get closer to the ultimate radiation efficiency limit. In addition, we use tunable components in the aperture to adapt currents over a wide band. Therefore, a conventional patch antenna is divided into smaller segments to have more freedom in exciting the radiating currents. Similar approach is also applied in [26], where a rectangular metal element over a ground plane was divided into four, closely-spaced smaller elements with narrow spacing. Each smaller element was fed separately with a port between the element and the ground. Adjacent elements had ports between them as well. These ports were replaced either with open connection or a capacitor.

In this paper, we modify the structure and utilize it in a mobile phone intended for 5G operation. Variable capacitors are used to achieve a wide-band operation over a frequency range of 3.3–4.2 GHz, and the antenna can excite two different linear polarizations by feeding the antenna from two different locations. An instantaneous bandwidth of 100 MHz is achieved

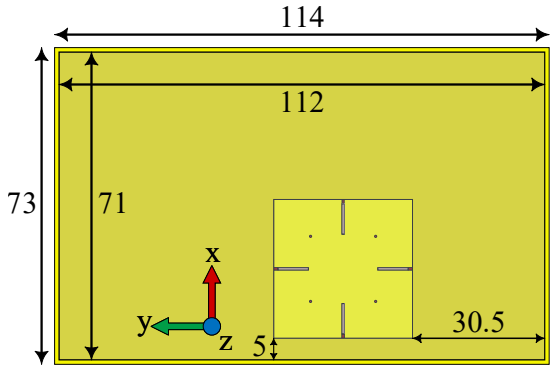

(a)

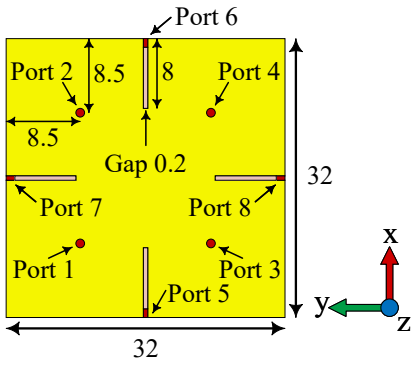

(b)

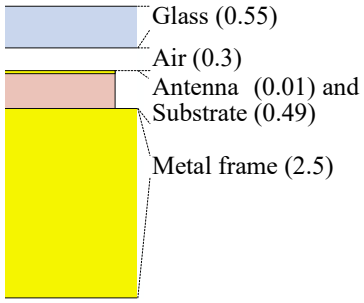

(c)

Fig. 1. Mobile phone dimensions and proposed antenna location (a) and dimensions (b), and the cross-section of the mobile phone and the antenna (c). All the dimensions are given in millimeters.

by tuning the variable capacitors. Thus, there are nine separate bands in total.

The antenna and mobile phone is shown in Fig. 1. The antenna location on the mobile phone is shown in Fig. 1a. The mobile phone model has an overall size of $73\,\text{mm} \times 114\,\text{mm} \times 3.8\,\text{mm}$. The phone model consists of a uniform metal body having a solid rim with a thickness of 1 mm, and inside the rim there is a glass ($\epsilon_\text{r} = 7.2$ and $\tan\delta = 0.025$) cover. The thickness of the glass is 0.55 mm as shown in Fig. 1c. The figure shows the cross-section of the mobile phone and the antenna. There is a 0.3 mm thick air gap between the antenna and the glass. The antenna copper and the PTFE ($\epsilon_\text{r} = 2.1$ and $\tan\delta = 0.009$) substrate have thicknesses of 0.01 mm and 0.49 mm, respectively. Thus, the antenna is only 0.55 mm thick. The phone body has a thickness of 2.5 mm.

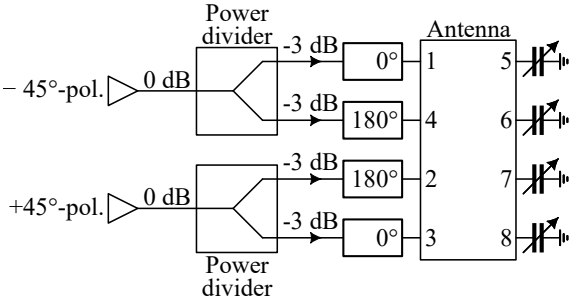

Fig. 2. Schematic of the representation of the antenna feeding

TABLE I
OPTIMIZED CAPACITANCE VALUES FOR PORTS 5–8 IN THE DIFFERENT BANDS.

Band (GHz)	Capacitance (pF)
3.3–3.4	2.38
3.4–3.5	1.95
3.5–3.6	1.68
3.6–3.7	1.48
3.7–3.8	1.32
3.8–3.9	1.19
3.9–4.0	1.09
4.0–4.1	1.00
4.1–4.2	0.92

The antenna element itself consists of a uniform metal patch having four feeding ports (1–4) connected to the ground. The feeding ports are simulated as discrete ports. The antenna has a size of $32\,\text{mm} \times 32\,\text{mm}$, and it has four slots that have a size of $0.2\,\text{mm} \times 8\,\text{mm}$. An ideal variable capacitor is placed at the outer edge of each slot to tune the resonant frequency. Ports 5–8 shown in Fig. 1b denote the place of variable capacitors which are considered ideal.

In [26], it was found that a differential feeding maximizes the radiation efficiency. Here we apply similar feeding scheme. Unlike in [26], here the structure is symmetric, and thus it is straightforward to achieve two orthogonal linear polarizations. Fig. 2 shows the schematic of the feeding for the antenna. Ports 1 and 4 are fed with an ideal 3-dB power divider, and port 4 is connected to a 180° an ideal phase shifter. Hence, the feeding is differential and resembles that of a dipole for example. This feeding excites a -45°-polarization, and $+45^\circ$-polarization is achieved by feeding ports 2 and 3 similarly. The two feeding ports exciting the polarizations are isolated since the coupling is below $-36\,\text{dB}$. Since the two ports are well isolated and excite orthogonal polarizations, the antenna can be used as a two-port MIMO antenna, or it can function as single antenna exciting any elliptical polarization by properly choosing the weights of the feeding ports.

The values of capacitors in ports 5–8 are chosen to maximize the total efficiency. The values are found through numerical optimization by modeling the antenna with its radiation

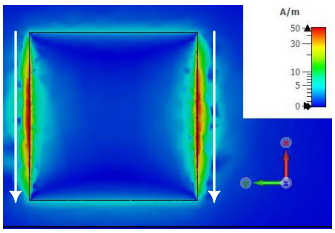

Fig. 3. The surface current distribution of the reference antenna at 3.158 GHz.

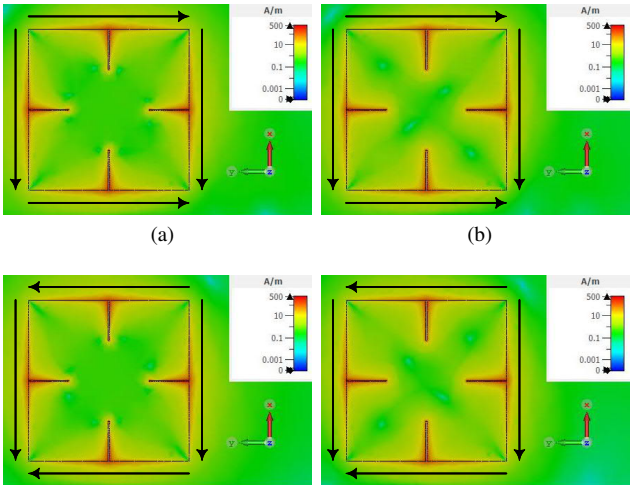

Fig. 4. The surface current distributions of the proposed antenna are shown for $+45°$ (a,b)- and $-45°$ (c,d)-polarized radiating modes at 3.3 GHz (a,c) and 4.2 GHz (b,d).

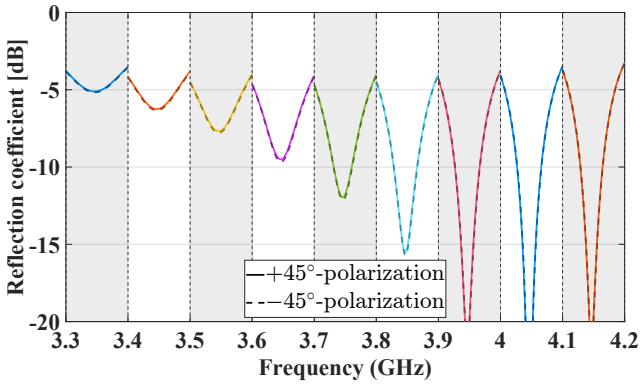

Fig. 5. Reflection coefficients of the proposed antenna for $+45°$- and $-45°$-polarized modes in the 100 MHz instantaneous bands

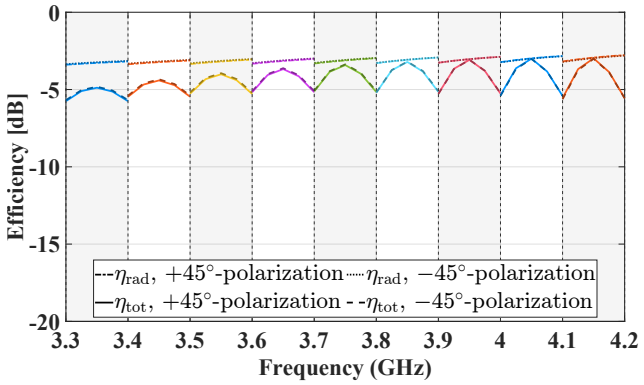

Fig. 6. Simulated radiation and total efficiencies of the proposed antenna for $+45°$- and $-45°$-polarized modes in the 100 MHz instantaneous bands.

and impedance matrices. Ports 1–4 are fed with the described feeding network, and the capacitor values in ports 5–8 are equal, for simplicity. Table I shows the optimized capacitances for the proposed antenna. The capacitor values vary between 0.91–3.07 pF, which is achievable with current commercial variable capacitors. For example, Skyworks SMV2020-079LF varactor diode [27] has a tunable capacitance range of 0.35–3.2 pF. The table shows that the capacitance decreases with increasing center frequency. The capacitance values in the lowest (3.3–3.4 GHz) and highest (4.1–4.2 GHz) bands are 2.38 pF and 0.92 pF, respectively.

Fig. 3 shows the current distribution of the X-polarized reference antenna at its center frequency of 3.158 GHz. The reference antenna is a conventional uniform patch antenna with a size of 32 mm $\times$ 32 mm, and it is located in the same place as the proposed antenna. The conventional antenna is fed with a single discrete port between the ground and the patch. The port is 6 mm away from the midpoint of the bottom edge.

Figs. 3 and 4 show that the current distributions of the proposed and the conventional patch antenna are different. The reference antenna has strong radiating currents at the opposite edges, whereas the proposed antenna has radiating currents at all the edges. For the prosed design, the currents at the opposite edges are in same phase which gives rise to X- and Y-polarized radiation. When the X- and Y-polarized radiation is combined, the polarization is either in $+45°$- or $-45°$-direction.

III. Results

The proposed multiport antenna has been simulated with CST Studio Suite, and the results are shown in Figs. 5, 6, and 8. Fig. 5 shows the reflection coefficient of the proposed antenna in the instantaneous 100 MHz bands. We can see that the reflection coefficient is between -4.1 dB and -3.3 dB at all the band edges. In higher bands, there are minimal reflection levels in the middle of the bands. For example, the reflection coefficient is below -10 dB in the 3.7–3.8 GHz band and in the higher bands. Thus, the antenna performance is limited by the relatively narrow bandwidth of matching at higher frequencies. However at lower frequencies, reflection is above -10 dB within the whole band. For example, the reflection coefficient is above -5.2 dB in the whole 3.3–3.4 GHz band. The reference antenna shows similar performance since its reflection coefficient (shown in Fig. 7a) is between -3.7 dB and -8.3 dB in the band of 3.108–3.208 GHz. The reference antenna is optimized for total efficiency in 100 MHz bandwidth, and hence, the minimum value of reflection coefficient is rather high.

Fig. 6 shows the radiation and total efficiency of the proposed antenna in the different bands and reveals that the

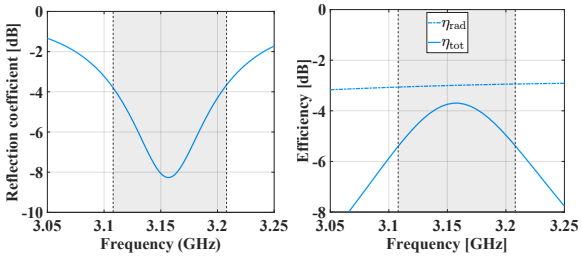

(a) (b)

Fig. 7. Simulated reflection coefficient (a) and radiation and total efficiencies (b) of the reference antenna.

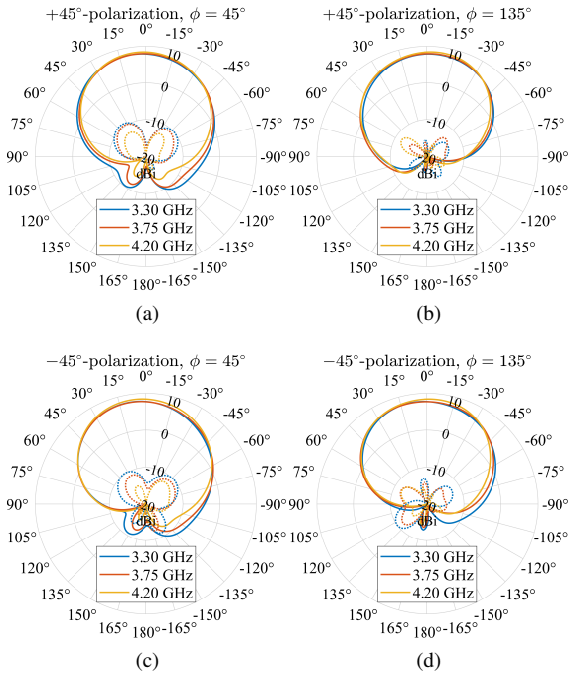

(a) (b) (c) (d)

Fig. 8. The co- and cross-polarized directivity patterns of the proposed antenna. Solid and dotted lines denote co- and cross-polarized components, respectively.

antenna is well optimized since both the lowest and highest band limit the minimum total efficiency, which is above -5.8 dB. At best, the total efficiency is -3.0 dB which is near the radiation efficiency. We can see that radiation efficiency is between -3.4 dB and -2.8 dB, which denotes that up to 2.8 dB improvement in total efficiency could be achieved with better matching. A single band of the proposed antenna is similar to that of the reference antenna 100 MHz band. The radiation and total efficiencies of the reference antenna are shown in Fig. 7. The radiation efficiency varies between -3.1 dB and -2.9 dB, and the minimum and maximum total efficiencies are -5.4 dB and -3.7 dB, respectively.

Furthermore, the results show that both the $+45°$- and $-45°$-polarized modes behave similarly as is expected based on the symmetry of the proposed antenna. The slight deviation in the results between the two polarizations is due to the asymmetrical placement on the phone itself. This asymmetry

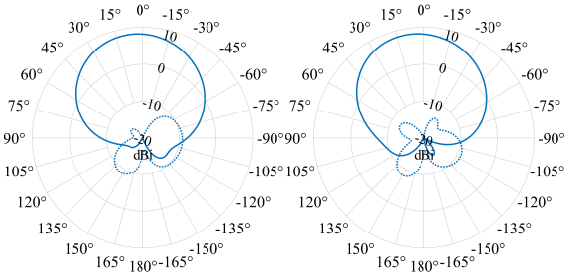

(a) (b)

Fig. 9. The directivity patterns of the reference antenna at 3.158 GHz at $\phi = 45°$ (a) and $\phi = 135°$ (b). Solid and dotted lines denote co- and cross-polarized components, respectively.

can also be seen in the radiation patterns which are shown in Fig. 8. Figure shows the directivity of the two polarizations at frequencies of 3.3 GHz, 3.75 GHz and 4.2 GHz thus including the lowest and the highest frequency of the band. The maximum directivity is between 7.9 dB and 8.5 dBi for the shown frequencies and the two polarizations. The cross-polarized field component is -9.1 dBi at maximum. Overall, the radiation patterns remain stable over the whole frequency range. The reference antenna patterns shown in Fig. 9 resemble those of the proposed antenna.

IV. Conclusion

In this paper, we have shown a novel dual-polarized patch antenna for sub-6 GHz having frequency reconfigurability from 3.3 GHz to 4.2 GHz. We have verified its operation with simulations. The antenna achieves frequency agility with four tunable capacitors, and the two feeding ports excite orthogonal polarizations. The antenna is located on the back cover of the phone. The achieved total efficiency is at least -5.8 dB in the whole band which is a good result due to the challenging design environment. The environment is challenging since the antenna is very thin (0.5 mm thick), and it is located under a lossy glass substrate.

Acknowledgment

The work was supported by Huawei Technologies Finland. The work of R. Kormilainen was supported by the Aalto ELEC Doctoral School.

References

[1] Q. Cai, Y. Li, X. Zhang, and W. Shen, "Wideband MIMO antenna array covering 3.3–7.1 GHz for 5G metal-rimmed smartphone applications," *IEEE Access*, vol. 7, pp. 142 070–142 084, 2019.

[2] Q. Chen, H. Lin, J. Wang, L. Ge, Y. Li, T. Pei, and C.-Y.-D. Sim, "Single ring slot-based antennas for metal-rimmed 4G/5G smartphones," *IEEE Transactions on Antennas and Propagation*, vol. 67, no. 3, pp. 1476–1487, 2019.

[3] L. Sun, Y. Li, Z. Zhang, and Z. Feng, "Wideband 5G MIMO antenna with integrated orthogonal-mode dual-antenna pairs for metal-rimmed smartphones," *IEEE Transactions on Antennas and Propagation*, vol. 68, no. 4, pp. 2494–2503, 2020.

[4] A. Singh and C. E. Saavedra, "Wide-bandwidth inverted-F stub fed hybrid loop antenna for 5G sub-6 GHz massive MIMO enabled handsets," *IET Microwaves, Antennas & Propagation*, vol. 14, no. 7, pp. 677–683, 2020.

[5] K. Rasilainen, R. Luomaniemi, A. Lehtovuori, J.-M. Hannula, and V. Viikari, "Ground clearance in smartphone antennas," in *2019 13th European Conference on Antennas and Propagation (EuCAP)*, 2019, pp. 1–5.

[6] D. Q. Liu, M. Zhang, H. J. Luo, H. L. Wen, and J. Wang, "Dual-band platform-free PIFA for 5G MIMO application of mobile devices," *IEEE Transactions on Antennas and Propagation*, vol. 66, no. 11, pp. 6328–6333, 2018.

[7] M. A. Fakih, A. Diallo, P. Le Thuc, R. Staraj, O. Mourad, and E. A. Rachid, "Optimization of efficient dual band PIFA system for MIMO half-duplex 4G/LTE and full-duplex 5G communications," *IEEE Access*, vol. 7, pp. 128 881–128 895, 2019.

[8] H. Gu, J. Wang, and L. Ge, "Circularly polarized patch antenna with frequency reconfiguration," *IEEE Antennas and Wireless Propagation Letters*, vol. 14, pp. 1770–1773, 2015.

[9] N. Nguyen-Trong, A. Piotrowski, and C. Fumeaux, "A frequency-reconfigurable dual-band low-profile monopolar antenna," *IEEE Transactions on Antennas and Propagation*, vol. 65, no. 7, pp. 3336–3343, 2017.

[10] Y.-M. Cai, K. Li, Y. Yin, S. Gao, W. Hu, and L. Zhao, "A low-profile frequency reconfigurable grid-slotted patch antenna," *IEEE Access*, vol. 6, pp. 36 305–36 312, 2018.

[11] W. Lin and H. Wong, "Polarization reconfigurable aperture-fed patch antenna and array," *IEEE Access*, vol. 4, pp. 1510–1517, 2016.

[12] K. M. Mak, H. W. Lai, K. M. Luk, and K. L. Ho, "Polarization reconfigurable circular patch antenna with a C-shaped," *IEEE Transactions on Antennas and Propagation*, vol. 65, no. 3, pp. 1388–1392, 2017.

[13] P.-Y. Qin, Y. J. Guo, Y. Cai, E. Dutkiewicz, and C.-H. Liang, "A reconfigurable antenna with frequency and polarization agility," *IEEE Antennas and Wireless Propagation Letters*, vol. 10, pp. 1373–1376, 2011.

[14] J. Hu and Z.-C. Hao, "Design of a frequency and polarization reconfigurable patch antenna with a stable gain," *IEEE Access*, vol. 6, pp. 68 169–68 175, 2018.

[15] Q. Xue, X. Y. Zhang, and C.-H. K. Chin, "A novel differential-fed patch antenna," *IEEE Antennas and Wireless Propagation Letters*, vol. 5, pp. 471–474, 2006.

[16] Z. Tang, J. Liu, Y.-M. Cai, J. Wang, and Y. Yin, "A wideband differentially fed dual-polarized stacked patch antenna with tuned slot excitations," *IEEE Transactions on Antennas and Propagation*, vol. 66, no. 4, pp. 2055–2060, 2018.

[17] S. Radavaram and M. Pour, "Reply to comments on "Wideband radiation reconfigurable microstrip patch antenna loaded with two inverted U-slots"," *IEEE Transactions on Antennas and Propagation*, vol. 68, no. 2, pp. 1216–1218, 2020.

[18] D. Yang, H. Zeng, R. Chen, J. Qu, Y. Wen, and S. Liu, "Four port compact multimode patch antenna system for vehicular application," in *2016 IEEE International Workshop on Electromagnetics: Applications and Student Innovation Competition (iWEM)*, 2016, pp. 1–3.

[19] K.-L. Wong, H.-J. Chang, J.-Z. Chen, and K.-Y. Wang, "Three wideband monopolar patch antennas in a Y-shape structure for 5G multi-input–multi-output access points," *IEEE Antennas and Wireless Propagation Letters*, vol. 19, no. 3, pp. 393–397, 2020.

[20] B. Li, J. Zhang, Y. Deng, Z. Zhou, and L. Sun, "Design of broadband circularly polarized patch antenna based on multi-feed method," in *2019 International Conference on Microwave and Millimeter Wave Technology (ICMMT)*, 2019, pp. 1–3.

[21] W. Duan, X. Y. Zhang, S. Liao, K. X. Wang, and Q. Xue, "Multiport power combining patch antenna with stable reflection coefficient and radiation pattern in six polarization states," *IEEE Transactions on Antennas and Propagation*, vol. 67, no. 2, pp. 719–729, 2019.

[22] B. Babakhani, S. K. Sharma, and N. R. Labadie, "A frequency agile microstrip patch phased array antenna with polarization reconfiguration," *IEEE Transactions on Antennas and Propagation*, vol. 64, no. 10, pp. 4316–4327, 2016.

[23] G. Jin, M. Li, and G. Zeng, "A simple differential-fed pattern reconfigurable dipole antenna," in *2018 International Applied Computational Electromagnetics Society Symposium - China (ACES)*, 2018, pp. 1–2.

[24] A. Derneryd and A. Lind, "Extended analysis of rectangular microstrip resonator antennas," *IEEE Transactions on Antennas and Propagation*, vol. 27, no. 6, pp. 846–849, 1979.

[25] D. Tayli and M. Gustafsson, "Physical bounds for antennas above a ground plane," *IEEE Antennas and Wireless Propagation Letters*, vol. 15, pp. 1281–1284, 2016.

[26] R. Kormilainen, J.-M. Hannula, T. O. Saarinen, A. Lehtovuori, and V. Viikari, "Realizing optimal current distributions for radiation efficiency in practical antennas," *IEEE Antennas and Wireless Propagation Letters*, vol. 19, no. 5, pp. 731–735, 2020.

[27] Skyworks Solutions, Inc. (2020) SMV2019 to SMV2023 series: Hyperabrupt junction tuning varactors. [Online]. Available: https://www.skyworksinc.com/-/media/SkyWorks/Documents/Products/201-300/SMV2019_to_SMV2023_Series_200074S.pdf